



## Graphene nano particles to improve lightning dissipation on transmission lines

I. Ramirez-Vazquez<sup>a\*</sup> • J. E. Salgado-Talavera<sup>b</sup> • E. Gaona-Estrada<sup>a</sup> •  
S. M. Rowland<sup>c</sup> • C. Manzanares-Diaz<sup>d</sup>

<sup>a</sup>Instituto Nacional de Electricidad y Energías Limpias (INEEL), 62490, Mexico

<sup>b</sup>Nissan Mexicana, 62578, Mexico

<sup>c</sup>The University of Manchester, M13 9PL, United Kingdom

<sup>d</sup>Comision Federal de Electricidad, 62755, Mexico

Received 08 03 2023; accepted 03 20 2024

Available 10 31 2024

**Abstract:** Lightning is the primary cause of outages for many high voltage transmission lines. One approach to reduce the frequency of these outages is the improvement of the grounding system using chemical ground enhancers to better disperse transient or fault currents into the soil. In this paper, the objective is to use graphene nano particles to improve the performance of commercial ground enhancers by exploration of 15 different commercial graphene nano particles used to reformulate 19 commercial ground enhancers and one natural ground enhancer. Incorporation of nano graphene particles is by high shear mixing method. The results show reduction in two of the commercial ground enhancers' resistivity values by a factor of 60. Moreover, lightning impulse tests show that the use of graphene reduce deterioration of the ground enhancer, which can occur after high current events, thereby prolonging its efficacy. Due to the superior electrical conductivity and chemical stability of the graphene, the reformulated ground enhancers improve short-term performance in managing lightning current impulses, and provide a solution, which is likely to perform better over long periods. However, the compatibility of the constituent parts of the formulation is critical to long-term performance.

**Keywords:** Ground enhancer, graphene nano particles, lightning, soil resistivity, chemical enhancer

\*Corresponding author.

E-mail address: iramirez@ineel.mx (I. Ramirez-Vazquez).

Peer Review under the responsibility of Universidad Nacional Autónoma de México.

## 1. Introduction

Many countries like Mexico have mentioned that lightning is the main cause of outages in power transmission and distribution lines, for example, USA (57%), Brazil (50-70%), Japan (70-80%), Denmark (57%), and Colombia (47-69%) have reported higher percentage rate of lightning outages according to Wareing (2016). When atmospheric discharges hit power lines, they produce travelling impulse voltages, which can cause flashover of insulators, and subsequent operation of protection regimes, which interrupt supply. Good earthing can minimize such events (back flashover), so grounding of the towers is vital to a reliable supply (Bayliss & Hardy, 2007; Shariatinasab, & Gholinezhad, 2019). Also, lightning-induced cause major issues on overhead distribution lines, due to its reduced insulation level compared with transmission lines (Soto & Perez, 2019). According to Sabnis and Jalaik (2023) for 230 kV transmission lines, a reduction in the tower footing grounding impedance from 80  $\Omega$  to 10  $\Omega$  resulted in the reduction of at least 66% on the amplitude of lightning overvoltage.

On the other side, soil frequency dependency is irrelevant at low frequencies and power frequencies under 100 Hz; which is a different consideration at higher frequencies. For example, CIGRE (CIGRE, 2019) suggests that for buried and transmission line earthing applications frequency dependency can be ignored for soil resistivities less than 300  $\Omega\cdot\text{m}$ , they recommend consider it for soil resistivities between 300 and 700  $\Omega\cdot\text{m}$ ; finally, they consider it mandatory for soils above 700  $\Omega\cdot\text{m}$ .

In the case of lightning induced voltages, CIGRE recommends taking into an account the soil-parameter frequency dependence when the range of soil resistivity is 2500  $\Omega\cdot\text{m}$ . and above; and neglected when is less than 2500  $\Omega\cdot\text{m}$ . In this regard, an improvement in soil-parameter with the use of graphene Nano Particles to improve chemical ground enhancers to better disperse transient or fault currents into the soil can be an important aspect for lightning dissipation on transmission lines, which is the objective of the research in this paper.

To reduce the harmful effects of lightning, the National Utility CFE (Comisión Federal de Electricidad) has implemented various solutions that have been analyzed and suggested jointly with the INEEL (Instituto Nacional de Electricidad y Energías Limpias). However, lightning remains as the primary cause of outages for power lines (CFE, 2012; CFE 2015).

Chemical ground enhancers improve the grounding system through a reduction in the contact resistance between the soil and the buried metallic element that is part of the grounding system. In addition, chemical ground enhancers provide a reduced resistance path for fault currents and lightning transients with the objective to dissipate them into the soil faster.

Due to the different soil types in Mexico such as clay, sandy clay, cultivated soil, sand, pure slate, and sandstone; is

common to find a wide range of soil resistivities, typically between 0.1  $\Omega\cdot\text{m}$  to 3,000  $\Omega\cdot\text{m}$  (Romualdo-Torres, 1996). Because of the problems associated with higher resistivities, the implementation of grounding systems using ground enhancement materials has been analyzed to evaluate potential benefits. Predesigned systems are considered for soil resistivities up to 1000  $\Omega\cdot\text{m}$ . When soil resistivity is higher than 1000  $\Omega\cdot\text{m}$  surge arresters are considered.

Commercial chemical enhancers are already used to decrease resistivity of the soil. For example, Galván et al. (2010), and Ahmad et al. (2010) showed a decrease in grounding resistance by a factor of between 0.18 and 0.8, and 0.08 and 0.67, respectively, although some “enhancing” compounds increased resistivity up to 13 times. In addition, the best chemical enhancement material identified by Ahmad et al. (2010) was NaCl, which is strongly corrosive and, due to its high solubility, is quickly swept away by groundwater. Typical enhancement materials used are palm kernel oil cake (PKOC), clays such as bentonite, graphite powder or carbon-based material, sodium chloride (NaCl), sodium thiosulfate ( $\text{Na}_2\text{S}_2\text{O}_3$ ), magnesium chloride ( $\text{MgCl}_2$ ), copper sulphate ( $\text{CuSO}_4$ ), and ammonium chloride ( $\text{NH}_4\text{Cl}$ ). According to manufacturers, these products increase conductivity up to approximately 200% or can decrease resistivity between 20 to 30 times lower than bentonite clay, which is the most natural enhancer used in power systems (Androvitsaneas et al., 2012). However, in the literature there is no evidence of resistivity measurements in commercial chemical enhancer after lightning events have occurred through a material.

Experience and analysis have shown that when lightning hits the earthed structure or tower of a power line, the risk of failure due to back flashover (arcing across an insulator from a grounded structure to a phase, because of the ground potential being raised) can be reduced if the grounding resistance is decreased. This is a big challenge for materials technology.

In recent years, researchers around the world have investigated the application of nano particles to improve the mechanical, thermal, and electrical properties of a wide range of materials. One of the main advantages of these nano particles is their large surface area per unit volume. Graphene is a highly promising and attractive nano material for a wide range of applications because of its distinctively high electrical and thermal conductivity, and because it is an electrochemically active material (Ferrari et al., 2015; Lee et al., 2014; Zhu et al., 2010). A roadmap highlights the steps to take graphene and related materials from a state of raw potential that might revolutionize multiple industries, however a challenge is the ability to produce graphene in large quantities at a reasonable cost (Ferrari et al., 2015). Graphene can also be combined with a wide variety of

inorganic materials such as metal oxides, which exhibit outstanding performance in applications such as super-capacitors (Lee et al., 2017; 2018), batteries, sensors, electromagnetic interference shielding (Lee et al., 2016), and photovoltaic applications (Rodriguez-Perez et al., 2017). When graphene and inorganic components are combined, synergistic effects can result at the molecular level and can create new properties distinct from the individual components (Low & Shon, 2018; Wu et al., 2012).

The experience and analysis in electrical engineering have shown that when a lightning hits the structure or tower of the power line, the risk of failure due to back flashover can be reduced if the grounding resistance is decreased, which since the point of view of materials science is a big challenge.

## 2. Materials and methods

As shown in Table 1, the measured thermal conductivity of graphene is in the range 3080 – 5300 W/mK at room temperature; compared to 190 W/mK for graphite (Kim et al., 2010); and the electrical conductivity of graphene is  $10^7$  S/m parallel to the surface and  $10^2$  S/m perpendicular to the surface. Exfoliated graphite has a conductivity of  $8.7 \times 10^4$  S/m (Blake et al., 2008). Commercial carbon black has lower electrical and thermal conductivities than both graphene and graphite. For comparison, nickel has a similar electrical conductivity to commodity graphene, however; the thermal conductivity of nickel is 19 to 33 times lower than graphene's.

Table 1. Electrical and thermal characteristics of graphene nano particles, graphite, and carbon black (Blake et al., 2008; Kim et al., 2010; Maquin et al., 2000; Pantea et al., 2001; Wypych, 2000).

Material	Electrical conductivity (S/m)	Thermal conductivity (W/K m)
Graphene	$10^7$ parallel to the surface	3080 – 5300
	$10^2$ perpendicular to the surface	
Graphite	$8.7 \times 10^4$ (exfoliated)	110-190
Carbon black	0.5-830	0.04
Nickel	$1.282 \times 10^7$	158

From these physical characteristics compared in Table 1, there is an expectation that the higher electrical and thermal conductivity of graphene nanoparticles will improve the conductivity of the ground enhancer materials beyond levels achievable with graphite or carbon black. Due to many advantages previously confirmed, such as a small weight percent of nano particles and a radical effect on the properties of a composite (up to 8% in weight giving an improvement of

1010 for electrical resistivity in a control epoxy) (XG Sciences, 2009), also, features that have been reported in Novoselov et al. (2012) and Krishnan et al. (2012) for graphene nano particles. Because of that, these materials were selected in this research to improve electrical conductivity of commercial chemical ground enhancers.

A review of commercial graphene and graphene oxide providers was carried out. It was found 38 different types of graphene are distributed by 7 suppliers; also 51 graphene oxide types were identified from 19 different suppliers. The main requirement for the selection of the nano particles was a high electrical conductivity and this characteristic was considered as the most important for the selection of the graphene nano particles. Additionally, it was analyzed if the commercial graphene nano particles were water-soluble because the identified commercial chemical enhancers were water-soluble. With this water compatibility between these components, the graphene nano particles and the commercial chemical enhancers, the possibility of mixing and dispersion was expected to be good. Also, in the data provided by the graphene suppliers, it was found that these nano particles are ethanol-soluble.

After an exhaustive analysis, 15 types of graphene were purchased for experimentation. In addition, 19 commercial chemical enhancers were identified, and these materials were also purchased. The graphene nano particles used for the preparation of the specimens are shown in Table 2.

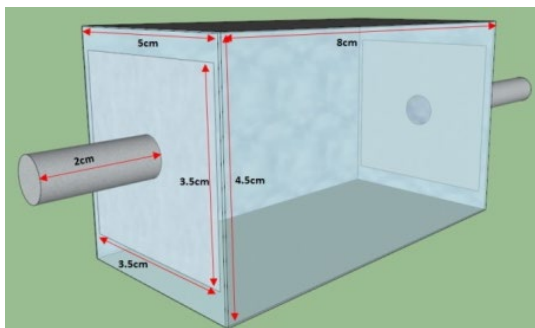
### 2.1. Experimental procedure

#### 2.1.1. Sample preparation

A laboratory high shear mixer was used to mix the ground enhancer material with the graphene nano particles. For the prepared blends, 50% weight of the 19 investigated commercial ground enhancers and one natural ground enhancer were each mixed with 37% weight of water, 3% weight of disperser aid (poly sodium styrene sulfonate), and 10% weight of graphene nano particles for about 25 minutes. Because of intellectual property, the chemical composition of the commercial ground enhancers is unknown. When each mixture was homogenous and free of lumps, it was poured into a container with dimensions of 8cm x 5.2cm x 4.5cm (length x width x height). The containers were made of an insulating material, and a pair of 3.5cm x 3.5cm stainless steel electrodes were attached with screws in opposite sides of the container to measure the resistivity of the sample as shown in Fig. 1(a) 225 specimens were prepared for laboratory testing. Over time, some samples showed evidence of shrinkage and developed open circuit measurements; these samples were physically compacted to get representative resistivity measurements. A schematic cross-section of the container, including electrodes, and one photograph of one sample are shown in Fig. 1(b).

Table 2. Graphene nano particle types and providers, with data provided by the suppliers.

Provider	Nano particle type	Electrical conductivity (S/m)	Thermal conductivity (W/mK)	Particle size	Manufacturing process
XG Sciences	H-15, M-15, and C-500.	3000 (parallel to the surface) 6 (perpendicular to the surface)	$10^7$ (parallel to the surface) $10^2$ (perpendicular to the surface)	Thickness of 6 to 15 nm, particle diameter of 15 $\mu\text{m}$ , surface area of 50-150m <sup>2</sup> /g.	Proprietary manufacturing process
Angstrong Materials	N008-100-P-40, N008-100-P-10, N008-100-N, N006-010-P, and N002-PDR	Information not available in the manufacturer’s web page.	Information not available in the manufacturer’s web page.	Thickness of 1 to 100 nm, particle diameter of 0.5 to 10 $\mu\text{m}$ , surface area of 40m <sup>2</sup> /g.	Information not available in the manufacturer’s web page.
Avanzare	AvanGRP	Exceptional in-plane electrical conductivity	High thermal conductivity	2x5 $\mu\text{m}$ and less than 10nm in thickness	Not specified
ID-nano	GOx	Information not provided by the manufacturer.	Information not provided by the manufacturer.	Information not provided by the manufacturer.	Proprietary manufacturing process
Xiamen Knano Graphene Technology	KNG-G5 KNG-150	12000	3000	Diameter of 5-20 $\mu\text{m}$ , thickness of 5nm	12000
Graphene Laboratories Inc.	AO-3, A0-4, and C1	Electrically conductive	Thermally conductive	Side of the particle between 5 to 25 $\mu\text{m}$ , thickness 5 to 30nm; surface area-60m <sup>2</sup> /g <sup>2</sup>	Not specified



(a)



(b)

Figure 1. (a) Schematic of the sample container showing electrodes in both sides Sample container and one sample prepared for laboratory evaluation and (b) Top view of one ground enhancer sample modified with graphene nano particles for laboratory evaluation.

### 2.1.2. Resistivity measurements

The ASTM Standard (ASTM G187, 2005) was used to evaluate the resistivity of the chemical ground enhancers using a Fluke 1625-2 instrument. Resistivity measurements were carried out periodically and the moisture content was calculated based on the weight of the sample; an example of a drying weight versus time is shown in Fig. 2. Fig 2 shows the impact of moisture being added after 2 months when the moisture content fell below 5%.

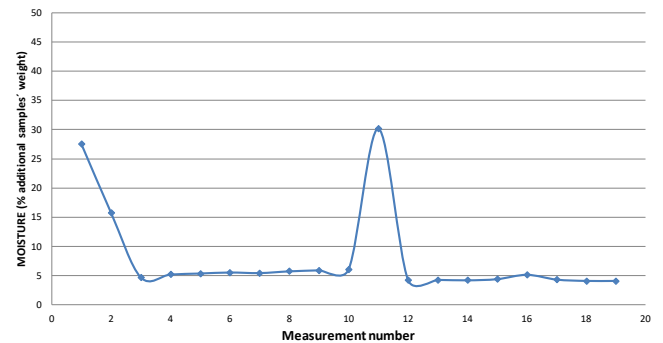


Figure 2. Behavior of the samples’ drying versus time by using the heating chamber (water was added to simulate rain after the moisture’s sample was lower than 5% of the sample’s weight).

### 2.1.3. Accelerated aging

Due to the number of specimens and because the drying (dehumidification) process of the samples at ambient temperature is very slow, samples were dried at a constant 50°C to 53°C. Drying at 50°C reduced the required time for the experiment by approximately half. This temperature does not degrade the chemical ground enhancers.

### 2.1.4. Impulse lightning current tests

When the moisture content of the samples was around 5% by weight, a group of five lightning impulses was applied to each specimen in order to simulate the phenomenon of lightning on the samples. The time between applications of each subsequent lightning impulse was 1 minute. Initially a lightning impulse current magnitude of 5kA using an  $8 \times 20\mu\text{S}$  waveform was applied; this magnitude was selected to cover the three stages of the soil ionization proposed by Liew and Darveniza (1974) in their dynamic model, consisting of three zones: no-ionization, ionization and de-ionization. In addition, Almeida and Barros (1996) proposed a soil ionization model based on the variable resistivity approach and a current greater than 4kA required to achieve ionization in the soil surrounding the earth electrode. However, in our experiments using such high currents, some samples exploded, as shown in Fig. 8. According to Almeida and Barros (1996), their model indicates that the resistance is constant until a critical current of 1kA is reached; after that breakdown occurs (Fig. 3). Therefore, to operate in the constant resistance stage and to obtain an ageing effect on the sample, the applied current magnitude was between 0.5kA and 1kA. In order to obtain these lightning impulse currents; the charging voltage of the lightning impulse current generator was increased gradually from 0.5 Volts to 6 Volts in five steps as shown in Table 6.

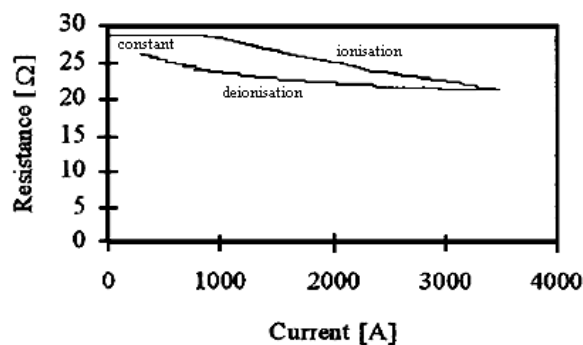


Figure 3. Impulse resistance as a function of current (Almeida & Barros, 1996).

The circuit used for the lightning impulse current test is shown in Fig. 4. The impulse generator has a capacitance of  $8\mu\text{F}$ , a maximum voltage of 40kVdc; a non-inductive current divider of  $0.005\Omega$ , and a non-inductive voltage divider.

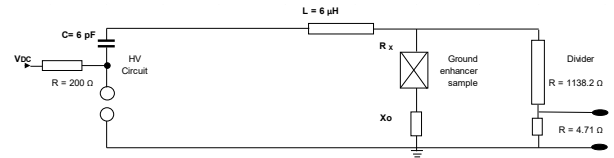


Figure 4. Schematic diagram of the lightning impulse current generator for the evaluation of chemical ground enhancers reinforced with nano particles.

The waveforms were measured by an oscilloscope TDS 5054b. Once this test was completed, 50ml of water was added to all samples to simulate the effect of rainfall during a storm. Thereafter, the samples remained in the heating chamber for monitoring their resistivity again.

### 2.1.5. Microscopy and elemental chemical analysis

To analyze the morphology and chemical constituents of the modified ground enhancer samples, a FE-SEM (Field Emission Scanning Electron Microscope) Hitachi S-5500 was used. The microscope is equipped with energy dispersive spectroscopy (EDX) spectrometer (Oxford Instruments Mod. X-act) and can measure the chemical composition of materials at the nanometer scale.

To reduce charge accumulation during observation of the ground enhancer samples, a small amount of material was deposited on a conductive double-sided carbon tape, previously attached to the sample stubs, and then introduced and observed in the microscope.

## 3. Results and discussion

### 3.1. Resistivity measurements

#### 3.1.1. Samples with laboratory grade graphene nano particles

Once the samples with and without laboratory grade graphene nano particles were manufactured, periodic measurements of resistivity were carried out to verify the performance of the samples as moisture is lost during the experiment. Resistivity measurements of the samples resulted in improvement factors for specimens reformulated with graphene nano particles up to 187 times when compared with the samples without nano particles (control samples). Because of limited space in this paper, here the focus is on the experimentation with industrial grade nano particles.

Table 3 shows resistivity improvement factors, obtained after drying, in specimens always greater than 10 times. Sample M1409 resulted in a factor of 187 times lower resistivity compared with the control. The matrix is the intensifier CGE 2 and the graphene nano particle is KNG-G5.

#### 3.1.2. Samples with industrial grade graphene nano particles

Once the samples with and without commercial graphene nano particles were manufactured, resistivity measurements were made immediately after sample manufacturing, and

then every day, except weekends to trace the resistivity as the samples dried. Table 4 shows a summary of the final measurements, when the samples were dry, with

improvement factor higher than 10 times. Many samples developed improvement factors lower than 10 times, and due to restrictions on space, these are not included here.

Table 3. Benchmarking of commercial ground enhancers modified with laboratory grade graphene nano particles obtained after drying. The improvement factor is the ratio of resistivity value compared to the control value with no graphene additive.

Rank order	Sample	Resistivity of the sample ( $\Omega \cdot \text{cm}$ )	Control sample resistivity ( $\Omega \cdot \text{cm}$ )	Improvement factor versus control	Graphene nano particle type	Matrix of commercial ground enhancer
1	M1409	770	144,822	187	KNG-G5	CGE 2
2	M1405	844	144,822	171	XGnP-H15	CGE 2
3	M1408	1,022	144,822	141	KNG-150	CGE 2
4	M604	504	29,963	59	G-IDT2 (Hz-ArH)	CGE 1
5	M601	620	29,963	48	G-IDT1 (Hz-ArH)	CGE 1
6	M1407	3,272	144,822	44	AO-4	CGE 2
7	M607	869	29,963	34	G-IDT3 (Asc-ArH)	CGE 1
8	M2003	400	9299	23	G-ID02	CGE 1
9	M1209	52,061	1,000,590	19	KNG-G5	CGE 17
10	M2105	413	7663	18	XGnP-H-15	CGE 2
11	M1004	5,724	61,388	10	GIDT-1	CGE 19

Table 4. Benchmarking of commercial ground enhancers modified with industrial grade graphene nano particles obtained after drying. The improvement factor is the ratio of resistivity value compared to the control value with no graphene additive.

Rank order	Sample	Resistivity of the sample ( $\Omega \cdot \text{cm}$ )	Control sample resistivity ( $\Omega \cdot \text{cm}$ )	Improvement factor versus control	Graphene nano particle type	Matrix of commercial ground enhancer
1	MP410	239.00	14,416.16	60.32	xGnP C500	CGE 3
2	MP320	282.07	14,416.16	51.11	KNG-G5	CGE 3
3	MP300	310.59	14,416.16	46.42	xGnP H-15	CGE 3
4	MP200	325.63	14,416.16	44.27	N008-100-P-10	CGE 3
5	MP400	328.68	14,416.16	43.86	xGnP M-15	CGE 3
6	MP430	367.18	14,416.16	39.26	C-1	CGE 3
7	MP274	1089.3	40,156.96	36.87	N008-100-N	CGE 19
8	MC303	48.70	1,626.86	33.40	xGnP H-15	CGE 1
9	MP210	452.53	14,416.16	31.86	N008-100-P-40	CGE 3
10	MP265	2384.27	66,030.49	27.69	N008-100-P-40	CGE 17
11	MP330	596.59	14,416.16	24.16	AO-4	CGE 3
12	MP220	651.67	14,416.16	22.12	N008-100-N	CGE 3
13	MP247	131.94	2,862.32	21.69	N006-010-P	CGE 2
14	MP219	12.31	247.69	20.12	N008-100-P-40	CGE 12
15	MP279	4102.26	72,753.05	17.73	N006-010-P	CGE 20
16	MP245	164.57	2,862.32	17.39	N008-100-P-40	CGE 2
17	MP267	3928.96	66,030.49	16.81	N006-010-P	CGE 17
18	MP310	1324.63	14,416.16	10.88	KNG 150	CGE 3
19	MP272	3780.44	40,156.96	10.62	N008-100-P-10	CGE 19
20	MP230	1385.78	14,416.16	10.40	N006-10-P	CGE 3

The CGE 12 (bentonite) was the material with the most significant response to dehydration inside the thermal chamber. Most samples with a matrix of bentonite, except sample MP 219, developed significant shrinkage, and cracked in several parts; because of the physical discontinuities that resulted from cracking in the material; these samples were useless for resistivity measurements. Despite sample with CGE 9 matrix material being prepared at the same time as the rest of the samples, it presented very high resistivity from the beginning of the experimentation, even with very high moisture content (almost 100% of the added water retained). In this sample, as soon as moisture was lost the resistivity increased yet more. After some time, several samples exceeded the measuring range of the device ( $> 299.9 \text{ K}\Omega$ ), these samples were prepared with matrix material: CGE 12 (bentonite; except MP219), CGE 9, CGE 10, CGE 8, CGE 7, CGE 14, CGE 16, and CGE 18. At this point of resistivity in the samples, it is considered that these ground enhancer materials are not a good choice, because in the field, when water/moisture is lost, the resistivity of these materials will be too high to be useful.

As a result of the experimentation on the commercial ground enhancers reformulated with industrial graphene nano particles it can be remarked that:

- The CGE 3 ground enhancer presented good performance with all nano particles except the AvanGRP nano particle type.
- The CGE 2 ground enhancer showed good interaction with the N008-100-P-40 and P-N006-010 nano particle types.
- The CGE 17 ground enhancer showed good interaction with the N008-100-P-40 and P-N006-010 nano particle types.
- The CGE 19 ground enhancer showed good interaction with the N008-100-P-10 and N008-100-N nano particle types.

It is important to mention that although samples prepared with matrix material CGE 12 (bentonite) and matrix CGE 20 presented improvement factors higher than 10; these samples lost moisture and physically cracked; hence, the resistivity values ultimately exceeded the measuring range of the instrument ( $> 299.9 \text{ K}\Omega$ ) before the end of the evaluation period. The samples prepared with CGE 3, CGE 17, and CGE 19 ground enhancers frequently suffered from discontinuity between the electrode and the material during the resistivity measurements, despite these samples being compacted; therefore, it is considered that these ground enhancers will be highly resistive and unsuitable in the drought season.

### 3.2. Lightning impulse current tests

The lightning performance of the samples that developed higher improvement factors is considered in this section. Due to the different manufacturing dates of the previous samples and to their history of ageing, new samples were prepared with two graphene nano particle, grades KNG-150 and XGnP-H15, and two ground enhancer materials previously identified. The analysis for the new samples was based on their cost, improvement factors, cost of the final formulation, and previous performance on lightning impulse testing with these matrixes' materials. This was done to plan the application in the field on transmission towers of a 400 kV transmission line. The samples were identified as MC300 to MC306 (for CGE 1 matrix) and MQ300 to MQ306 (for CGE 2 matrix). All samples were prepared on the same day. The purpose of this test was to evaluate the behavior of these materials and possible degradation or aging because of high current densities. Several lightning current waveforms were discharged through these materials, and it was observed that in samples incorporating nano graphene particles is easier to dissipate the impulse lightning current.

Once the first set of 5 lightning impulse current tests was completed on a sample, it was re-hydrated using 50ml of tap water to simulate a rainfall as mentioned Section 2.1.4; thereafter, samples remained in the heating chamber. In this second part of the experimentation, the samples were kept at  $25^\circ\text{C}$  and a relative humidity of 30% before resistivity measurements were made; resistivity measurements were made up to the point where the moisture was less than 5% by weight in the samples. In the third part of the experiment, a second set of 5 lightning impulse current tests was performed on the samples. All samples, except those consisting of MC303 and MC306, ended up with higher resistivity values after the lightning impulse current test than before.

The charging voltage magnitude of the impulse generator capacitors were the same for the first and the second set of 5 lightning impulse current tests applied to the samples MC300 to MC306 and MQ300 to MQ306. In addition, the results indicate that samples MC303, MC306, MQ303 and MQ306 were those that developed high current values at low charging voltages; this means that these samples are more conductive than other samples. The resistivity measurements made after the first and the second set of lightning impulse tests applied to the samples MC300 to MC306 and MQ300 to MQ306 are shown in Fig. 5 and 6. Also, Table 5 indicates the average lightning current magnitudes applied to samples MQ300 to MQ306 during the lightning impulse tests.

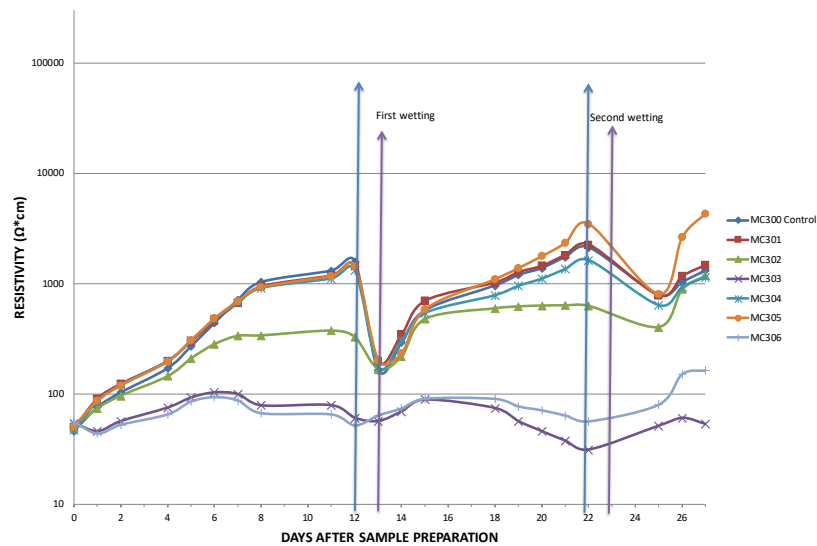


Figure 5. Resistivity of the MC300 Control sample and MC301 to MC306 samples modified with graphene nano particles.

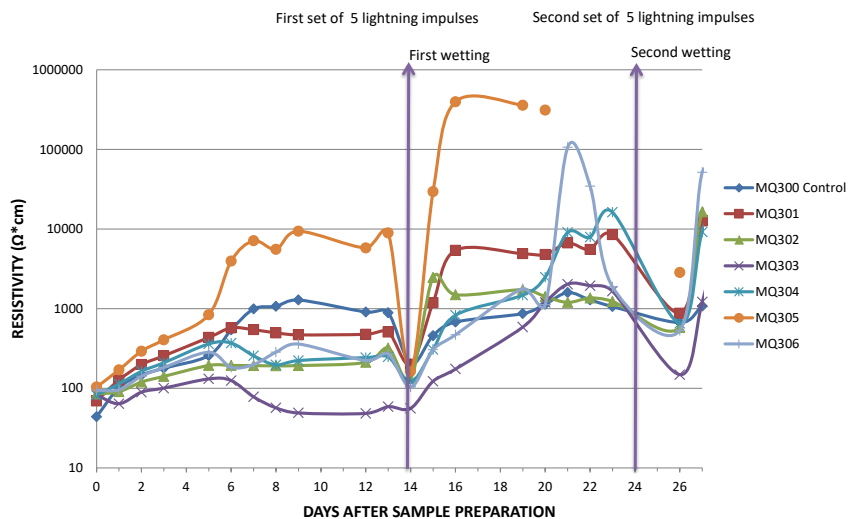


Figure 6. Resistivity of the MQ300Control sample and MQ301 to MQ306 samples modified with graphene nano particles.

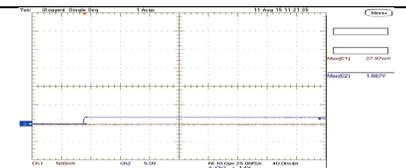
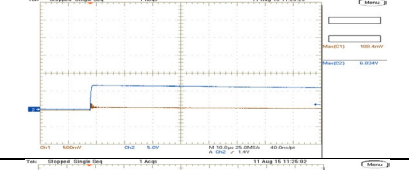
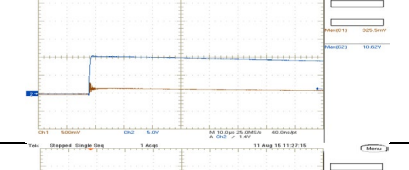
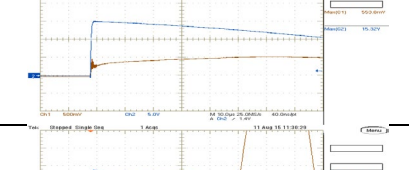
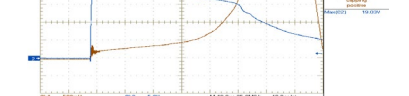
As can be seen in Figures 5 and 6, there is an upward trend in the resistivity values of all the samples in time. Therefore, a change in the conductive properties of the material would be expected over time, when subjected to an operating condition of lightning at field. This behavior is attributed to the influence of the lightning impulse current tests performed on the samples.

The waveforms obtained during the lightning impulse current tests for sample MQ305 in the second set is shown in Table 6. It should be noted that this sample exploded in the last lightning test because a higher impulse current was developed (higher than 3.017 kA was registered in the oscilloscope), probably because a higher ionization on the sample. Due to space reasons, these waveforms are not shown for the rest of the samples.

Table 5. Average lightning impulse current magnitudes applied to MQ300 Control and MQ301 to MQ306 samples: first, and second set of lightning impulse tests. Note: \*Sample exploded at the last lightning impulse.

Sample	Set of 5 lightning impulses	Average current (kA)	Standard deviation
MQ300	First set	506	238
	Second set	312	107
MQ301	First set	332	235
	Second set	152	121
MQ302	First set	690	388
	Second set	447	270
MQ303	First set	752	335
	Second set	671	346
MQ304	First set	467	379
	Second set	263	208
MQ305	First set	230	187
	Second set	121	76*
MQ306	First set	511	339
	Second set	372	260

Table 6. Lightning impulse current waveforms obtained during testing of the MQ305 sample in the second set of tests.

Sample	Charging voltage in the impulse generator (V)	Current (kA)	Waveform
MQ305	0.5	0.02343	
	2.5	0.158	
	4.0	0.273	
	6.0	0.462	
	7.5	>3.017	

The thermal image of the MQ305 sample it is shown in Fig. 7. It is noted that an increase in the temperature of the chemical enhancer is appreciated in the electrodes' trajectory.



Figure 7. Thermal image of MQ305 sample after lightning impulse current test; it is note that the sample exploded during the last impulse test.

To observe the effect of possible aging in the samples, resistivity measurements were carried out for each sample just before the first and second set of lightning impulse tests, and

after one week after the second set. The resistivity measurements are presented in Table 7, and Fig. 8.

As shown in Fig. 8, lightning impulse current tests increase resistivity. After the completion of the lightning impulse current testing, the MC303 and MC306 samples showed improvement factors of 33 and 8; the rest of the samples from the same batch had improvement factors lower than 2. Before lightning impulse test the improvement, factors were 68 and 38 respectively for these samples; as can be noticed, the testing modified resistivities of these samples.

After lightning impulse tests, the samples lost moisture due to the high value of the impulse current; consequently, their resistivity is increased. On the other side, the contact resistance between the chemical enhancer with graphene particles are smaller than chemical enhancer without graphene nano particles. While the distance between chemical enhancer with graphene nano particles is shorter on average, the conductivity is relatively higher. Obviously, the chemical enhancer with graphene nano particles has shorter distance, so it takes better effect on reducing grounding resistance. That can be one of the reasons why chemical enhancer with graphene nano particles has higher conductive than chemical enhancer without graphene nano particles.

Considering the principle under lightning, the critical breakdown field strength ( $E_c$ ) is another important factor besides the resistivity (Androvitsaneas et al., 2014; Hu et al., 2012).

Table 7. Resistivities of the samples MC300 Control and MC301 to MC306; and MQ300 Control and MQ301 to MQ306: before the first and second set of lightning impulse tests, and after one week after the second set of impulse tests.

Matrix of commercial ground enhancer	Graphene nano particle type	Sample	Resistivity ( $\Omega \cdot \text{cm}$ )		
			Before first set of 5 lightning impulses	Before second set of 5 lightning impulses	One week after the second set of 5 lightning impulses
CGE 1	None	MC300 Control	1580	2129	1627
	XGnP-H15	MC301	1439	2250	1728
	XGnP-H15	MC302	326	627	1147
	XGnP-H15	MC303	61	31	49
	KNG-150	MC304	1331	1628	1316
	KNG-150	MC305	1440	3473	4250
CGE 2	None	MQ300 Control	908	1064	1448
	XGnP-H15	MQ301	477	8515	14177
	XGnP-H15	MQ302	212	1232	10681
	XGnP-H15	MQ303	48	1658	16552
	KNG-150	MQ304	243	16269	13057
	KNG-150	MQ305	5796	Open circuit	Open circuit
	KNG-150	MQ306	223	1885	34614

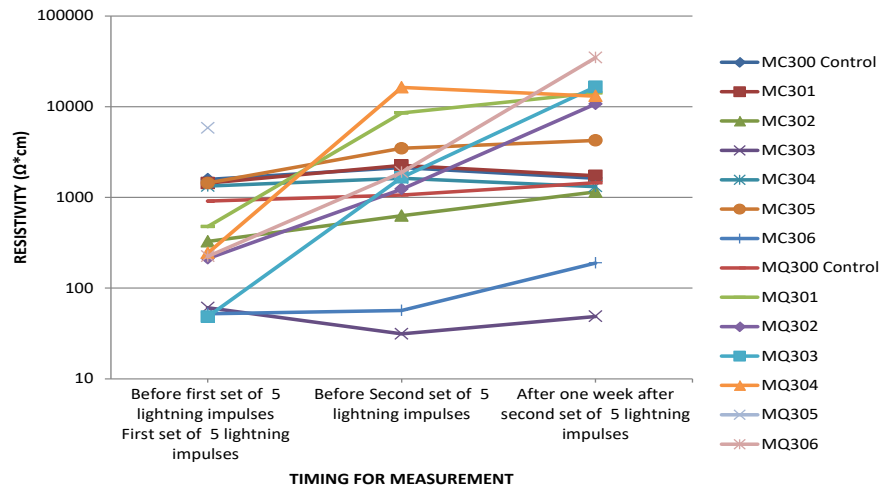


Figure 8. Resistivities of the samples MC300 Control and MC301 to MC306; and MQ300 Control and MQ301 to MQ306 just before the first and second set of lightning impulse tests, and after one week after the second set of impulse tests; from Table 5.

It is well known that the electric field strength follows the Eq. 1.

$$Ec = \rho J \tag{1}$$

Where:

$\rho$  = is the resistivity of the chemical enhancer

$J$  = is the current density which diffusing in the chemical enhancer.

Under lightning condition, chemical enhancer with graphene nano particles is ionized and this is an important factor to the effect of reducing grounding impedance.

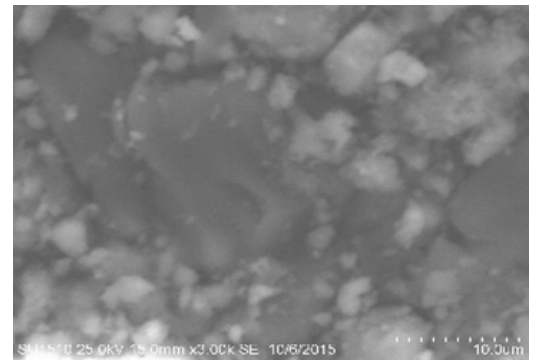
The  $E_c$  of the chemical enhancer with graphene nano particles is higher than the chemical enhancer without graphene nano particles. This is because the chemical enhancer with graphene nano particles is dense and has shorter distance between micro and nano particles that conform it. Also, it is harder for the charged micro particles to accumulate enough energy to cause ionization due to their higher gaps (distance between particles).

It is shown, according to Fig. 6, that resistivity of the chemical enhancers with graphene nano particles increased after lightning impulse application and it can affect its long-term stability.

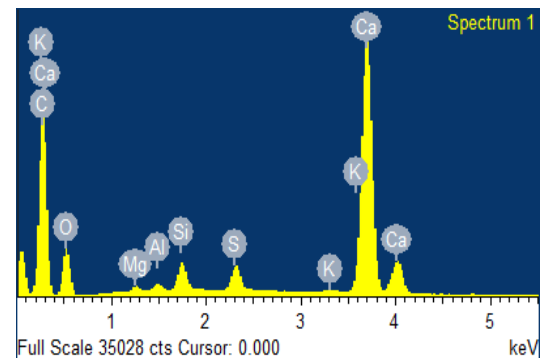
### 3.3. Microscopy analysis of the modified ground enhancer

Micrographs and EDX analysis obtained for the ground enhancers with high improvement factors, after lightning impulse current testing. A difference was found between the elements that form CGE1 samples and CGE2 samples. The micrographs were obtained for the ground enhancers, which

obtained the highest improvement factors; the micrographs are shown in Fig. 9 to 11.

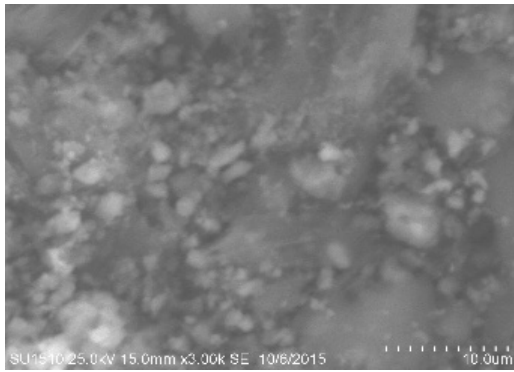


(a)

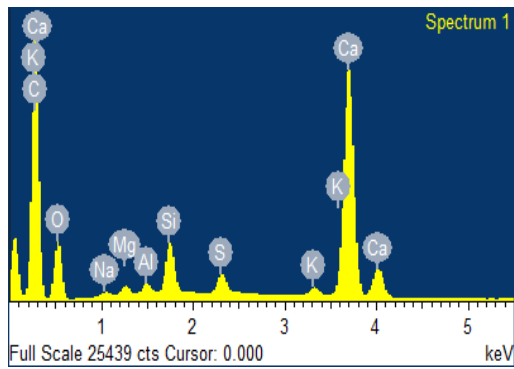


(b)

Figure 9. (a) Electron microscopy of the sample and (b) Elemental analysis obtained by EDX of the MC300 control sample.

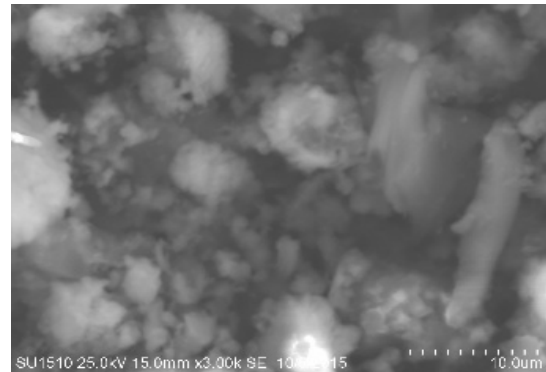


(a)

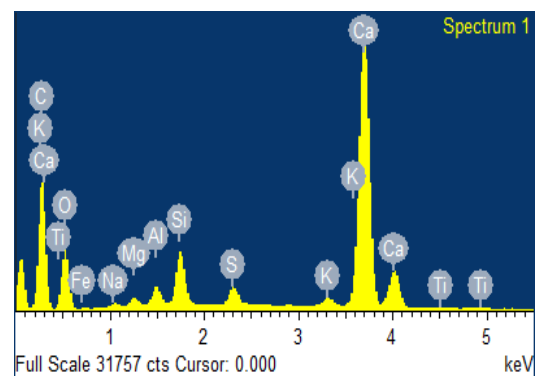


(b)

Figure 10. (a) Electron microscopy of the sample and (b) Elemental analysis obtained by EDX of the MC303 sample modified with xGNP H-15 graphene nano particles.



(a)



(b)

Figure 11. (a) Electron microscopy of the sample and (b) Elemental analysis obtained by EDX analysis of the MC306 sample modified with KNG-150 graphene nano particles.

### 3.4. Elemental chemical analysis

This analysis was done in different two matrices ground enhancer materials, CGE 1 and CGE 2, modified by two types of graphene nano particles x-GNP H15, and KNG-150. The analysis of chemical elements by SEM and EDAX analysis is shown in Table 8. From the elemental analysis can be seen that samples prepared with the commercial ground enhancer matrix CGE 2 modified with two different graphene nano particles (MQ303 and MQ306) were found to contain higher concentrations of chlorine and sodium (around 40% and 45% respectively); probably due to high levels of NaCl in the formulation. Also, it was observed that as time passed, a white layer formed on the top of these samples. The white layer was analyzed as 100% carbon. This indicates a low compatibility of graphene nano particles with the CGE 2 ground enhancer. This agrees with observations by Hong et al. (2012), who noted that upon exposure to aqueous NaCl solutions, graphene oxide precipitates.

Samples with CGE 1 ground enhancer modified with graphene nano particles (MC303 and MC306) contain high levels of carbon according to their elemental analysis, which indicates a good compatibility of its constituents with graphene nano particles. It can be seen clearly in Table 6, that the dominant elements in the CGE 1 samples are carbon and oxygen, while CGE 2 samples are formed with sodium and chlorine. This analysis illustrates the probable cause of the corrosive nature of the CGE 2 samples observed during the laboratory experimentation.

According to Wu et al. (2012), graphene can form a structure with an electron conductive network and shortest paths for transporting ions. Also, graphene can act as a two-dimensional conductive network for building a three-dimensional interconnected porous conductive network to improve the electrical conductivity and charge transport. This can be one of the possible reasons about why graphene nano particles are improving the conductivity of the ground enhancer material.

Table 8. Summary of EDAX analysis of commercial ground enhancers modified/unmodified with graphene nano particles.

Element	MC300 Control (weight %)	MC303 (modified with xGnP H-15 graphene nano particles) (weight %)	MC306 (modified with KNG-150 graphene nano particles) (weight %)	MQ300 Control (weight %)	MQ303 (modified with x-GnP H-15 graphene nano particles) (weight %)	MQ306 (modified with KNG-150 graphene nano particles) (weight %)
C	68.75	78.39	58.86	-	-	-
O	28.16	19.89	34.31	17.29	22.89	10.83
Na	-	0.19	0.43	39.38	36.91	45.36
Mg	0.3	0.25	0.54	0.66	0.78	-
Al	0.21	0.14	0.75	1.92	1.69	0.65
Si	0.66	0.48	1.58	5.5	5.29	1.39
S	0.34	0.17	0.31	-	-	-
K	0.02	0.02	0.08	0.14	-	-
Ca	1.57	0.47	2.08	0.31	0.19	0.28
Fe	-	-	1.05	-	1.77	-
Ti	-	-	0.01	-	-	-
Cl	-	-	-	34.65	29.37	40.12
Nd	-	-	-	0.14	0.1	0.22
Mo	-	-	-	-	0.77	1.15
Sb	-	-	-	-	0.25	-

### 3.5. Planned field installation

Based on the obtained results in the experimentation; the best chemical enhancer modified with graphene nano particles will be selected for field installation.

For a field installation higher amount of graphene nano particles are needed; so, the main problem is to get several tens of kilograms of nano particles. The other problem is its higher cost.

For the mixing process in the field, an industrial mixer and a power source (electric power generator) are needed to mix this type of materials. This is a big challenge; to mix properly graphene nano particles with chemical enhancer and to obtain a good dispersion; so, a proper mixer should be found. On the other hand, it is necessary to establish the proportions of water and material so that the resulting compound has a colloidal consistency, to conform electrodes of 10 cm of diameter and depths of 2 and 3 m; that is in order to differentiate if the installation civil works of the grounding system can be optimized.

For resistivity, soil moisture is one of the fundamental parameters that influence the behavior of grounding resistance, which is directly related to rainfall levels, as well as the type and composition of the soil (porosity, compaction, etc.), so it will be important to measure ground resistivity in dry

and wet seasons of the improved chemical enhancer with graphene nano particles.

Finally, the operators must use safety equipment consisting of dust mask, glasses, gloves and appropriate work clothing.

### 4. Conclusions

The Commercial ground enhancers reformulated with industrial grade graphene nano particles and laboratory grade graphene nano particles resulted in increased conductivities by factors of 60 and 187 respectively. However, not all the 19 evaluated commercial ground enhancers have a good interaction with the graphene nano particles; the compatibility depends strongly on the materials of which the ground enhancer is made. The supply chain for graphene is continually changing, and whilst the cost and quality of graphene nano particles used in these samples (laboratory grade) is presently higher than the industrial grades available due to its purity, number of layers, production method, etc., it is the core properties which are of most concern.

It was observed that nano graphene particles reduce the increases of resistivity, which results after the application of lightning impulse current on ground enhancers, in some cases by an order of magnitude. This is likely to be due to improved

dissipation of the lightning impulse current, and associated heating due to its electrical and thermal conductivity. The longevity of such improvements depends on the compatibility of the constituent parts. In the cases studied here, high levels of NaCl in the formulation reduced compatibility and may also be expected to increase levels of metallic corrosion.

The lightning impulse current testing developed and reported here is not currently in any standard as a design tool for ground enhancement materials. This test was found to be critical in understanding the stability of the system. Therefore, it is recommended that this be included in Utility standards as a requirement for chemical enhancers, to make sure that they do not age prematurely.

Following these laboratory results, a field installation is now being planned to test a system based on the industrial grade graphene nano particles combined with commercial ground enhancers.

### Conflict of interest

The authors have no conflict of interest to declare.

### Acknowledgements

The authors gratefully acknowledge the contributions of Octavio Félix-Sandoval, Manuel Ávila-Rodríguez, Antonio Martínez-Díaz, and Evaristo Merino-Mares for their contribution in this project.

### Funding

This work was supported by the CONACYT-FINNOVA (Consejo Nacional de Ciencia y Tecnología- Fideicomiso del Fondo Sectorial de Innovación), Fund #224798, and the INEEL-FICYDET (Instituto Nacional de Electricidad y Energías Limpias-Fideicomiso para el Apoyo a la Investigación Científica y Desarrollo Tecnológico).

### References

Ahmad, W. W., Rahman, M. A., Jasni, J., Ab Kadir, M. Z. A., & Hizam, H. (2010). Chemical enhancement materials for grounding purposes. In *2010 30th International Conference on Lightning Protection (ICLP)* (pp. 1-6). IEEE.

<https://doi.org/10.1109/ICLP.2010.7845836>

Almeida, M. E., & De Barros, M. C. (1996). Accurate modelling of rod driven tower footing. In *Proceedings of ESMO'95-1995 IEEE 7th International Conference on Transmission and Distribution Construction, Operation and Live-Line Maintenance* (pp. 70-73). IEEE.

<https://doi.org/10.1109/TDCLLM.1995.485038>

American Society for Testing and Materials (2005). *ASTM G187 Standard test method for Measurement of Soil Resistivity Using the Two-Electrode Soil Box Method*. West Conshohocken, PA, USA, ASTM. <https://www.astm.org/g0187-18.html>

Androvitsaneas, V. P., Gonos, I. F., & Stathopoulos, I. A. (2012). Performance of ground enhancing compounds during the year. In *2012 International Conference on Lightning Protection (ICLP)*, Vienna, Austria. (pp. 1-5). IEEE.

<https://doi.org/10.1109/ICLP.2012.6344356>

Androvitsaneas, V. P., Gonos, I. F., & Stathopoulos, I. A. (2014). Transient impedance of grounding rods encased in ground enhancing compounds. In *2014 International Conference on Lightning Protection (ICLP)*, Shanghai, China. (pp. 359-363). IEEE.

<https://doi.org/10.1109/ICLP.2014.6973148>

Bayliss, C.R. & Hardy, B.J. (2007). *Transmission and Distribution Electrical Engineering*. Newnes, Oxford.

Bayliss, C., & Hardy, B. (2007). *Transmission and Distribution Electrical Engineering*. Newnes, Oxford.

Blake, P., Brimicombe, P.D., Nair, R.R., Booth, T.J., Jiang, D., Schedin, F., Ponomarenko, L.A., Morozov, S.V., Gleeson, H.F., Hill, E.W., Geim, A.K. & Novoselov, K.S. (2008). Graphene-Based Liquid Crystal Device. *Nano Letters*, 8(6), 1704-1708. <https://doi.org/10.1021/nl080649i>

CIGRE (2019). *Impact of soil-parameter frequency dependence on the response of grounding electrodes and on the lightning performance of electrical systems*. WG C4.33 Pub. C4 TB 781.

CIGRE (2019). *Impact of soil-parameter frequency dependence on the response of grounding electrodes and on the lightning performance of electrical systems*. WG C4.33 Pub. C4 TB 781.

- Comision Federal de Electricidad (2015). *CFE Summary of Failures in Transmission Lines 2010-2014*. Mexico. (in Spanish)
- Comision Federal de Electricidad (2012). *CFE Outages, Statistics, and Relevant Works in Transmission Lines 2011*. Mexico. (in Spanish)
- Ferrari, A.C., Bonaccorso, F., Fal'ko, V., Novoselov, K.S., Roche, S., Bøggild, P., Borini, S., Koppens, F.H.L., Palermo, V., Pugno, N., Garrido, J.A., Sordan, R., Bianco, A., Ballerini, L., Prato, M., Lidorikis, E., Kivioja, J., Marinelli, C., Ryhänen, T., ... & Kinaret, J. (2015). Science and technology roadmap for graphene, related two-dimensional crystals, and hybrid systems. *Nanoscale*, 7(11), 4598-4810. <https://doi.org/10.1039/C4NR01600A>
- Galván, A., Pretelin, G., & Gaona, E. (2010). Practical evaluation of ground enhancing compounds for high soil resistivities. In *2010 30th International Conference on Lightning Protection (ICLP)*, Cagliari, Italy. (pp. 1-4). IEEE. <https://doi.org/10.1109/ICLP.2010.7845889>
- Hong, B. J., Compton, O. C., An, Z., Eryazici, I. & Nguyen, S. T. (2012). Successful Stabilization of Graphene Oxide in Electrolyte Solutions: Enhancement of Biofunctionalization and Cellular Uptake. *ACS Nano*, 6(1), 63-73. <https://doi.org/10.1021/nn202355p>
- Hu, W., Yu, S., Cheng, R., & He, J. (2012). A testing research on the effect of conductive backfill on reducing grounding resistance under lightning. In *2012 International Conference on Lightning Protection (ICLP)*, Vienna, Austria. (pp. 1-4). IEEE. <https://doi.org/10.1109/ICLP.2012.6344300>
- Kim, H., Abdala, A. A., & Macosko, C. W. (2010). Graphene/polymer nanocomposites. *Macromolecules*, 43(16), 6515-6530. <https://doi.org/10.1021/ma100572e>
- Krishnan, D., Kim, F., Luo, J., Cruz-Silva, R., Cote, L.J., Jang, H.D. & Huang, J. (2012). Energetic graphene oxide: Challenges and opportunities. *Nano Today*, 7(2), 137-152. <https://doi.org/10.1016/j.nantod.2012.02.003>
- Lee, C., Chang, H., & Jang, H. D. (2017). Preparation of CoFe<sub>2</sub>O<sub>4</sub>-graphene composites using aerosol spray pyrolysis for supercapacitors application. *Aerosol and Air Quality Research*, 19(3), 443-448. <http://dx.doi.org/10.11629/jpaar.2017.3.31.033>
- Lee, C., Chang, H., & Jang, H. D. (2018). Preparation of Core-Shell Structured Iron Oxide/Graphene Composites for Supercapacitors Application. *Particle and aerosol research*, 14(3), 65-72. <http://dx.doi.org/10.11629/jpaar.2018.14.3.065>
- Lee, J., Jang, H. Y., Jung, I., Yoon, Y., Jang, H. J., Lee, H., & Park, S. (2014). Facile Synthesis of Pt Nanoparticle and Graphene Composite Materials: Comparison of Electrocatalytic Activity with Analogous CNT Composite. *Bulletin of the Korean Chemical Society*, 35(7), 1973-1978. <https://doi.org/10.5012/BKCS.2014.35.7.1973>
- Lee, S. H., & Oh, I. K. (2016). Hybrid Carbon Nanomaterials for Electromagnetic Interference Shielding. *Composites Research*, 29(4), 138-144. <https://doi.org/10.7234/composres.2016.29.4.138>
- Liew, A. C., & Darveniza, M. (1974). Dynamic model of impulse characteristics of concentrated earths. In *Proceedings of the Institution of electrical Engineers* (Vol. 121, No. 2, pp. 123-135). IET Digital Library. <https://doi.org/10.1049/piee.1974.0022>
- Low S. & Shon Y.S. (2018). Molecular interactions between pre-formed metal nanoparticles and graphene families. *Advances in Nano Research*, 6(4), 357-375. <https://doi.org/10.12989/anr.2018.6.4.357>
- Maquin, B., Goyhénèche, J. M., Derré, A., Trinquescoste, M., Chadeyron, P., & Delhaès, P. (2000). Thermal conductivity of submicrometre particles: carbon blacks and solid solutions containing C, B and N. *Journal of Physics D: Applied Physics*, 33(1), 8. <https://doi.org/10.1088/0022-3727/33/1/302>
- Novoselov, K. S., Colombo, L., Gellert, P. R., Schwab, M. G., & Kim, K. A. J. N. (2012). A roadmap for graphene. *nature*, 490(7419), 192-200. <https://doi.org/10.1038/nature11458>
- Pantea, D., Darmstadt, H., Kaliaguine, S., Sümmchen, L., & Roy, C. (2001). Electrical conductivity of thermal carbon blacks: Influence of surface chemistry. *Carbon*, 39(8), 1147-1158. [https://doi.org/10.1016/S0008-6223\(00\)00239-6](https://doi.org/10.1016/S0008-6223(00)00239-6)
- Rodriguez-Perez, M., Villanueva-Cab, J., & Pal, U. (2017). Evaluation of thermally and chemically reduced graphene oxide films as counter electrodes on dye-sensitized solar cells. *Advances in nano research*, 5(3), 231. <https://doi.org/10.12989/anr.2017.5.3.231>

Romualdo-Torres, C. (1996). *Lightning Performance of Transmission and Distribution Lines*. The University of Manchester (United Kingdom).

Sabnis, S. & Jalaik, V. (2023). *Study on impact of lightning in hybrid cable – overhead lines*. Master's Degree in Energy Engineering, Department of Energy Engineering, Aalborg University.

Shariatinasab, R., & Gholinezhad, J. (2019). The effect of grounding system modeling on lightning-related studies of transmission lines. *Journal of Applied Research and Technology*, 15(6).  
<https://doi.org/10.1016/j.jart.2017.06.003>

Soto, E., & Perez, E. (2019). Lightning-induced voltages on overhead lines over irregular terrains. *Electric Power Systems Research*, 176, 105941.  
<https://doi.org/10.1016/j.epsr.2019.105941>

XG Sciences (2009). *Technical specification of XG Sciences*. XG Sciences. <https://nanoplore.ca/sds-tds/>

Wareing, B. (2016). Experience with Application of TLAs on 400 kV Line in Scottish Highlands. In *Insulator News and Market Report*, 2(112), 38-44. <https://www.inmr.com/experience-with-application-of-tlas-on-400-kv-line/>

Wu, Z. S., Zhou, G., Yin, L. C., Ren, W., Li, F., & Cheng, H. M. (2012). Graphene/metal oxide composite electrode materials for energy storage. *Nano Energy*, 1(1), 107-131.  
<https://doi.org/10.1016/j.nanoen.2011.11.001>

Wypych, G. (2000). *Handbook of fillers*, (2nd Edition). ChemTec Publishing. Toronto, Canada. <https://doi.org/10.1016/B978-1-895198-91-1.50001-4>

Zhu, Y., Murali, S., Cai, W., Li, X., Suk, J. W., Potts, J. R., & Ruoff, R. S. (2010). Graphene and graphene oxide: synthesis, properties, and applications. *Advanced materials*, 22(35), 3906-3924.  
<https://doi.org/10.1002/adma.201001068>